



Effect of polymerization conditions on physicochemical properties of gold-like lustrous films of organic solvent soluble 3-methoxythiophene oligomers

Minako Kubo¹ · Hiroataka Doi¹ · Ryota Saito¹ · Kenta Horikoshi¹ · Satoru Tsukada¹ · Katsuyoshi Hoshino¹

Received: 11 March 2021 / Revised: 6 April 2021 / Accepted: 7 April 2021 / Published online: 20 May 2021
© The Society of Polymer Science, Japan 2021

Abstract

Solution-cast films of ClO_4^- -doped oligo(3-methoxythiophene) exhibit a luster similar to that of metallic gold; however, the effects of synthetic conditions on the physicochemical properties of the above oligomer and its films remain underexplored. To bridge this gap, this study examines how these properties are affected by (i) the time required to add the oxidant solution to the monomer solution (t_a) and (ii) the polymerization time (t_p) for oligomer synthesis, revealing that oligomer molecular weight, film conductivity, and the amount of edge-on lamellar crystallites increase with decreasing t_a and/or increasing t_p . Given that the crystallinity of edge-on lamellar structures, together with film surface roughness, strongly influences film specular reflectance, the obtained results are expected to facilitate the fabrication of conductive oligo(3-methoxythiophene) films with tunable color and metal-like luster for diverse applications.

Introduction

Poly(3-alkylthiophene)s and their derivatives are soluble and readily processable conductive polymers that exhibit (electro)chemical stability and hold great promise for the construction of organic light-emitting diodes [1, 2], field-effect transistors [3], photovoltaic cells [4, 5], and solid-state sensors [6]. The most prominent feature of these polymers is the formation of quasicrystals in the solid (powder and film) state, i.e., the solid polymers comprise self-assembled lamellar crystallites in an amorphous matrix. Among the methods commonly used to prepare poly(3-alkylthiophene)s (e.g., oxidative polymerization [7], electropolymerization [8], organometallic reactant-induced polycondensation [9]), oxidative polymerization is particularly well suited for large-scale production, as this one-pot, cheap, and easy-to-implement technique relies on the

simple addition of an oxidant solution to an alkylthiophene solution. The physicochemical properties of the obtained polymers, such as regioregularity, polymerization degree, and polydispersity, are affected by the oxidant addition rate (ν), polymerization time (t_p), and polymerization temperature (T). In particular, molecular weight [10] and regioregularity [11, 12] were reported to increase with decreasing ν and increasing t_p (up to $t_p \approx 2$ h), whereas T has been reported to be positively correlated with molecular weight [12] and the width of its distribution [11] and negatively correlated with regioregularity [13] and crystallinity [14].

Previously, we synthesized a high-molecular weight oligomer of 3-methoxythiophene and studied the properties of its solutions and solution-cast films [15–17], revealing that unlike solid poly(3-alkylthiophene) films, oligo(3-methoxythiophene) (O3MeOT) films had a gold- or bronze-like color and demonstrating that lamellar crystals (edge-on lamellar crystallites) were formed in the solid films of both polymers. The crystallites formed by O3MeOT were more compact than those of poly(3-alkylthiophene)s and thus exhibited a greater refractive index and extinction coefficient, which gives rise to luster. However, the effects of polymerization conditions such as oxidant addition rate, polymerization time, and polymerization temperature on the physicochemical properties of O3MeOT remain unknown. Given the importance of these effects for the modulation of the optical and structural film properties, we herein probe

Supplementary information The online version contains supplementary material available at <https://doi.org/10.1038/s41428-021-00496-w>.

✉ Katsuyoshi Hoshino
k_hoshino@faculty.chiba-u.jp

¹ Department of Materials Science, Graduate School of Engineering, Chiba University, Chiba, Japan

the influence of oxidant addition rate and polymerization time on the properties of O3MeOT films, demonstrating that the above parameters affect oligomer molecular weight, solution-cast film color, and lamellar crystallite structure in these films.

Experimental

Materials

3-Methoxythiophene (>98%; Fujifilm Wako Pure Chemical Co., Osaka, Japan) was polymerized by oxidation with $\text{Fe}(\text{ClO}_4)_3 \cdot n\text{H}_2\text{O}$ (anhydrous salt content =70.7%; Fujifilm Wako Pure Chemical). Acetonitrile (>99.7%; Kanto Chemical, Tokyo, Japan), nitromethane (>98.0%; Tokyo Chemical Industry, Tokyo, Japan), and methanol (99.8%; Kanto Chemical, Tokyo, Japan) were used as supplied. The glass plate (S1225, Matsunami Glass, Osaka, Japan) was cleaned by 10-min sonication in acetone (>99.5%; Kanto Chemical) prior to use.

Oligomer synthesis

O3MeOT was prepared as reported elsewhere [15–17]. Briefly, a solution of 3-methoxythiophene (0.57 g) in acetonitrile (50 mL) was placed in a 300-mL three-necked flask, deaerated by 30-min nitrogen bubbling upon stirring at 350 rpm, and supplemented with a solution of $\text{Fe}(\text{ClO}_4)_3 \cdot n\text{H}_2\text{O}$ (3.54 g) in acetonitrile (50 mL) prepared by 20-min ultrasonication. Instead of the addition rate v , the addition time t_a was used as a variable ($t_a = 0.08, 10, 30,$ and 60 min). The resulting solution was stirred at 20 °C for a certain period of time ($t_p = 10, 30, 60,$ and 120 min) and suction-filtered through a membrane filter (pore size = 0.1 μm). The filter cake was washed vigorously with methanol at least three times, and the resulting deep blue powder was vacuum-dried (AVO-250NB, As One, Osaka, Japan) at 50 °C for 1.5 h to yield ClO_4^- -doped O3MeOT. Samples prepared under different conditions were denoted as O3MeOT(x, y), where x and y stand for t_a (min) and t_p (min), respectively.

Coating solution and film preparation

Typically, O3MeOT (0.010 g) was dissolved in nitromethane (0.99 g, 0.87 mL) upon 90-min stirring at 22 °C, and the resulting solution was aged for 1 day [16], applied to a glass plate (15 mm \times 25 mm \times 1.1 mm), and dried under ambient conditions to afford a film. The quantity of the applied solution equaled 70 or 100 μL . Films prepared from O3MeOT(x, y) were denoted as Film(x, y).

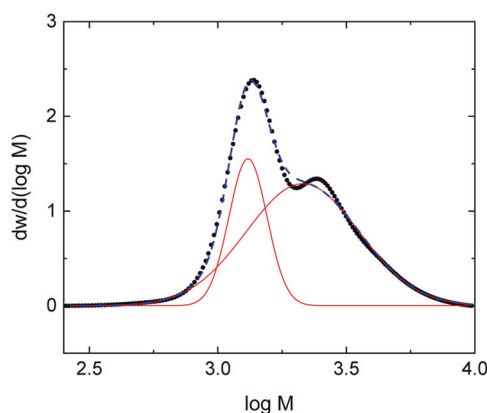


Fig. 1 Differential molecular weight distribution curve (filled circles) of O3MeOT (0.08, 60), w = concentration fraction. Solid red curves show the most likely distributions obtained by deconvolution of experimental data. The broken blue line represents the fitted cumulative molecular weight distribution. Deconvolution was carried out using the Gaussian function of OriginPro 2020 software (OriginLab Corp., Northampton, MA, USA)

Characterization

Details pertaining to the instruments and methods used for oligomer and film characterization can be found in the Supplementary Information.

Results and discussion

Oligomer molecular weight

Figure 1 shows the differential molecular weight distribution curve of O3MeOT(0.08, 60), revealing that M ranged from 500–10,000. As the experimental values (filled black circles) formed a subpeak on the high-molecular weight side of the main peak, the obtained curve was deconvoluted (solid red curves) using double Gaussian fitting. The distribution curves of other oligomers are presented in Supplementary Fig. S1. In all cases, the molecular weights derived from the two fitting curves differed by a factor of ~ 2 , which indicated the presence of both nonaggregated oligomers and their π -dimers in 1-methyl-2-pyrrolidone [18–20]. This finding agreed with our previous work [16], where viscosity and UV–vis absorption measurements were used to show that O3MeOT(0.08, 60) may form a π -dimer in nitromethane, and would have presented direct evidence of π -dimers. Table 1 lists the weight-averaged molecular weights (M_w), number-averaged molecular weights (M_n), and polydispersity indices ($\text{PDI} = M_w/M_n$) obtained herein, revealing that as M_w and M_n represent the average physical properties of oligomer nonaggregates and π -dimers, they did not depend on t_a and t_p . To properly evaluate the

Table 1 Molecular weight data of oligomers prepared under different conditions

Entry	Oligomer	$10^{-3}M_w$	$10^{-3}M_n$	DPI	$10^{-3}M_p$
1	O3MeOT (0.08, 10)	1.96	1.53	1.28	1.32
2	O3MeOT (0.08, 30)	2.13	1.68	1.27	1.38
3	O3MeOT (0.08, 60)	2.09	1.65	1.27	1.38
4	O3MeOT (0.08, 120)	2.01	1.61	1.25	1.42
5	O3MeOT(10, 60)	1.80	1.41	1.28	1.23
6	O3MeOT(30, 60)	1.89	1.45	1.31	1.23
7	O3MeOT(60, 60)	1.93	1.46	1.32	1.20

M_w , weight average molecular weight; M_n , number average molecular weight, DPI polydispersity index, M_p , molecular weight corresponding to the main peak in the differential molecular weight distribution curve

molecular weight of O3MeOT molecules, one should use the nonaggregate molecular weight as an index. However, in Fig. 1, the fitted cumulative molecular weight distribution curve (broken line) derived from the sum of the two fitting curves for the nonaggregate and π -dimer does not fully agree with the measured values. Therefore, the molecular weight M_p , corresponding to the maximum of the main peak of the differential molecular weight distribution, was tentatively defined as the molecular weight of the nonaggregate and was shown to increase with t_p and decrease with t_a (last column of Table 1). The former trend was also reported for the polymerization of alkylthiophenes [10, 12], although the latter trend was different from that observed for poly(alkylthiophene)s. Facchinatto et al. synthesized poly(3-hexylthiophene) by the dropwise addition of a $FeCl_3$ solution into a 3-hexylthiophene solution ($t_a = 7, 17,$ and 180 min) and found that molecular weight was positively correlated with t_a , although the origin of this dependence was not described [10]. Torres et al. synthesized poly(3-octylthiophene) via the dropwise addition of an $FeCl_3$ solution into a 3-octylthiophene solution ($t_a = \sim 0, 15, 60,$ and 180 min) and concluded that t_a did not directly affect the molecular weight distribution of the resulting polymer [11]. The effect of t_a on M_p and regioregularity is discussed in the next section.

Note that the difference in M_p values listed in Table 1 corresponds to only one or two 3-methoxythiophene units. Therefore, although it could not be treated strictly, this difference was considered meaningful for the following reasons. D'Agnillo et al. performed a round-robin experiment using various polyethylenes and determined the standard deviations of molecular weight [21]. For a relatively small PDI (e.g., $PDI = 2.2$) and an unbranched structure, the standard deviations for M_w and M_n corresponding to repeatability on the same instrument within one laboratory were obtained as 3 and 5%, respectively. In our previous work, O3MeOT(0.08, 60) was shown to have an

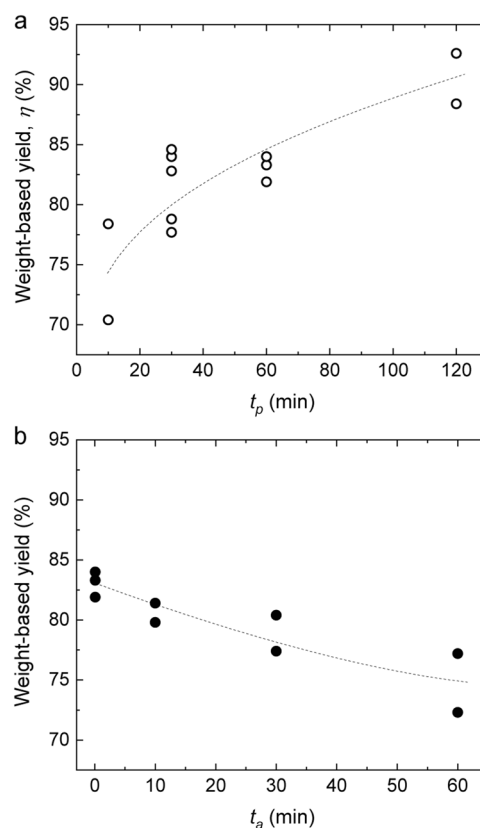


Fig. 2 Effects of t_p (a) and t_a (b) on the weight-based yield of O3MeOT. In **a** t_a was held constant at 0.08 min, and in **b** t_p was held constant at 60 min

unbranched structure [15]. In addition, Table 1 shows that the PDI values of the O3MeOT samples were sufficiently small. The GPC measurement was repeated three times using a polystyrene standard to determine the standard deviation of elution time as 0.02 min, which corresponds to a molecular weight of ~ 40 . This value is the standard deviation of the chromatograph for a standard sample. As the chromatographic standard deviation for all oligomers was expected to be roughly the same as above, the net standard deviation of their molecular weight was expected to be close to 80. This value was $\sim 5\%$ of the oligomer M_p and agreed well with that estimated by D'Agnillo et al.

The effects of t_p and t_a on M_p were in line with those on the weight-based synthetic yield, η . Figure 2a shows that in the case of O3MeOT(0.08, t_p) ($t_p = 10, 30, 60,$ and 120 min), η monotonically increased with t_p , which was interpreted as an increase in the proportion of oligomers insoluble in acetonitrile due to the concomitant increase in M_p . It should also be noted that the preparation of oligomers involved their purification by washing with methanol. As methanol is known to dissolve low-molecular-weight components [13], the increase in M_p with t_p may reflect the decrease in the proportion of low-molecular-weight components due to their removal during washing. Figure 2b

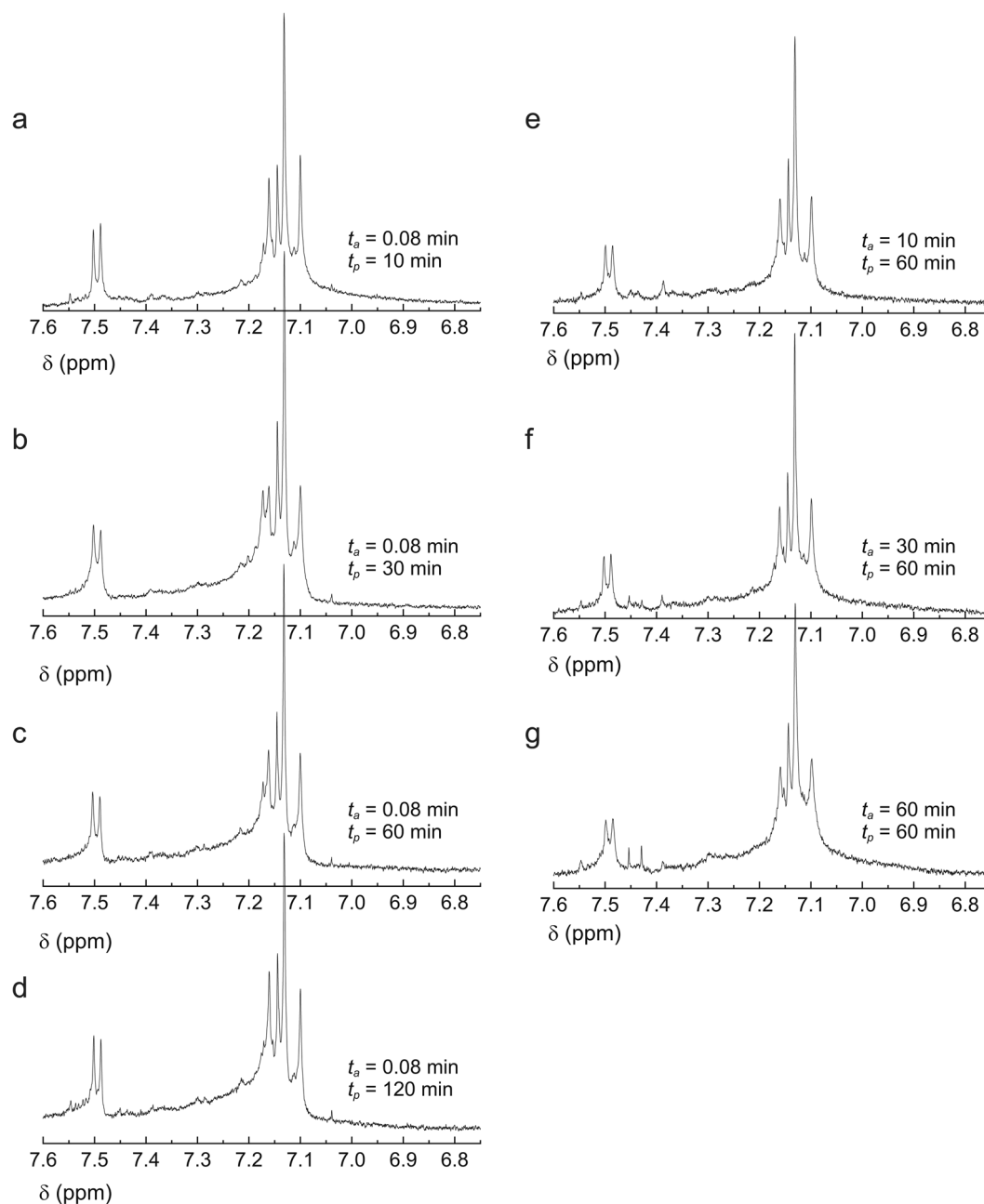


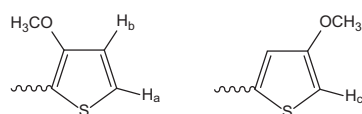
Fig. 3 ^1H NMR spectra (aromatic region) of **a** O3MeOT(0.08, 10), **b** O3MeOT(0.08, 30), **c** O3MeOT(0.08, 60), **d** O3MeOT(0.08, 120), **e** O3MeOT(10, 60), **f** O3MeOT(30, 60), and **g** O3MeOT(60, 60)

shows that for O3MeOT(t_a , 60) ($t_a = 0.08, 10, 30,$ and 60), η decreased with t_a , indicating that the content of low-molecular-weight components concomitantly increased for the reason described above.

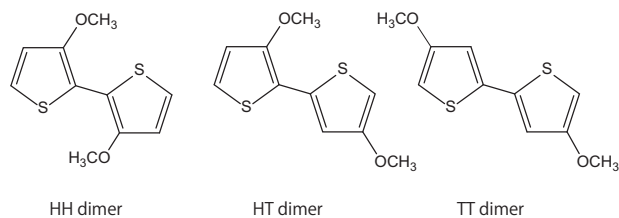
Oligomer regioregularity

The ^1H NMR spectra (DMSO- d_6) of the oligomers listed in Table 1 (Fig. 3) reveal several hydrogen peaks at position 4 of the thienyl rings. According to the previously reported ^1H

NMR spectra of poly(3-alkoxythiophene)s [22, 23] and poly(3-alkylthiophene)s [9, 24–26], the multiple signals at 7.13–7.17 ppm were assigned to protons associated with nonterminal thienyl rings, indicating that O3MeOT specimens had a regiorandom chain structure. For example, in Fig. 3c, the above signals comprised a major peak at 7.13 ppm and three minor peaks at 7.14, 7.16, and 7.17 ppm, which were assigned to HT-HT, TT-HT, HT-HH, and TT-HH triad configurations, respectively. Here, HT, TT, and HH represent head-to-tail, tail-to-tail, and head-to-



Scheme 1 Terminal ring configurations for O3MeOT



Scheme 2 Three regioisomeric bis(methoxy)-2,2'-bithiophenes

head diads, respectively. The doublet centered at 7.49 ppm and the signal at 7.10 ppm were assigned to protons H_a and H_c , respectively (Scheme 1) [9, 24, 25]. H_b was attributed to the doublet that was expected to be present between 7.10 and 7.13 ppm [24] but was not clearly observed, probably because of the overlap with the signals at 7.10 and 7.13 ppm or because of masking by the main peak at 7.13 ppm.

The intensity of the signal due to the proton at the 4-position on the nonterminal thienyl ring was in the order of HT-HT \gg TT-HT > HT-HH > TT-HH for all the spectra. Barbarella et al. calculated the electron densities at carbons C-2, C-4, and C-5 of 3-methoxythiophene and its radical cation, showing that the electron density at C-2 exceeded that at C-5 seven- to eightfold [27]. Moreover, the electron density at C-4 was one to two orders of magnitude smaller than that at C-2. Considering the large directing power of the methoxy group, one can assume that C-2 carbons are linked together and that HH dimers are preferentially formed in the early stage of polymerization (Scheme 2). In addition, dimers have a lower oxidation potential than monomers and are therefore more readily oxidized. Thus, carbon C-5 of the resulting oxidized HH dimer attacks carbon C-2 of the monomer to produce the HT linkage, and this process is repeated to form an HT oligomer with one HH linkage. However, this mechanism does not account for the effect of t_a . When t_a is small (i.e., at a high oxidation potential), numerous 3-methoxythiophene radicals are rapidly formed at the onset of polymerization and non-selectively couple with each other [12] to afford HT and TT dimers in addition to the HH dimer (Scheme 2) [27]. The subsequent dimer + monomer and dimer + dimer couplings afford regiorandom oligomers. However, as the methoxy group has a much larger directing power than alkyl groups [11, 27], the HT-HT configuration is expected to be dominant. In fact, for $t_a = 0.08$ min (Fig. 3a–c), we observed a signal of the TT-HH configuration at 7.17 ppm, while this signal was very weak for longer t_a (Fig. 3e–g). Even for $t_a = 0.08$ min, the TT-HH signal was hardly

observed when t_p was increased (Fig. 3d). This behavior suggests that the concentration of radicals at a given time decreased with increasing t_p , which resulted in more selective polymerization.

As mentioned above, the nonselective coupling of 3-methoxythiophene likely to proceed at $t_a = 0.08$ min produces three regioisomeric dimers (HT, HH, and TT). Barbarella et al. synthesized the HT, HH, and TT dimers of 3-(alkylsulfanyl)thiophene and showed that the oxidative polymerization of HT and HH dimers produced oligomers, while polymers were formed from TT dimers. Theoretical calculations on these dimers showed that the TT dimer and its radical cation are highly reactive because of their two equivalent high-electron-density ends and are polymerized to give high-molecular-weight products. Based on this report, one can infer that more TT dimers are formed at $t_a = 0.08$ min than at larger t_a values. The higher concentration of TT dimers should increase the probability of polymerization between them to produce higher-molecular-weight oligomers, which may be the reason for the negative correlation of M_p with t_a shown in Table 1.

External appearance of films

Figure 4 shows the images of films prepared from the oligomers listed in Table 1. The films in Fig. 4a–d were prepared using a coating solution volume of 70 μ L, whereas the films in Fig. 4e–h were prepared using a volume of 100 μ L, as in this case (large t_a), the viscosity of the coating solution was overly low to allow the uniform formation of films at a volume of 70 μ L. All films except for Film(0.08, 10) strongly reflected the scale of a stainless steel ruler standing perpendicular to the film surface and thus exhibited high specular reflectance. Film(0.08, 10) showed poor film-forming properties compared to other films and experienced delamination, which could be ascribed to a small M_p . Visual observations showed that Film(0.08, 10) and Film(0.08, 60) had relatively strong yellowish hues, which was subsequently confirmed by colorimetric measurements.

Film color measurements

Figure 5 shows the a^* , b^* chromaticity diagrams of films, revealing that b^* , which indicates yellow color intensity, decreased with increasing t_p (Fig. 5a). The hue angle (h) defined in Eq. (1) decreased with t_p , i.e., the red color intensity concomitantly increased (Fig. 5b).

$$h = \tan^{-1}(b^*/a^*) \quad (1)$$

The cause of this color deepening may be assumed to be an increase in the extent of perchlorate doping and/or

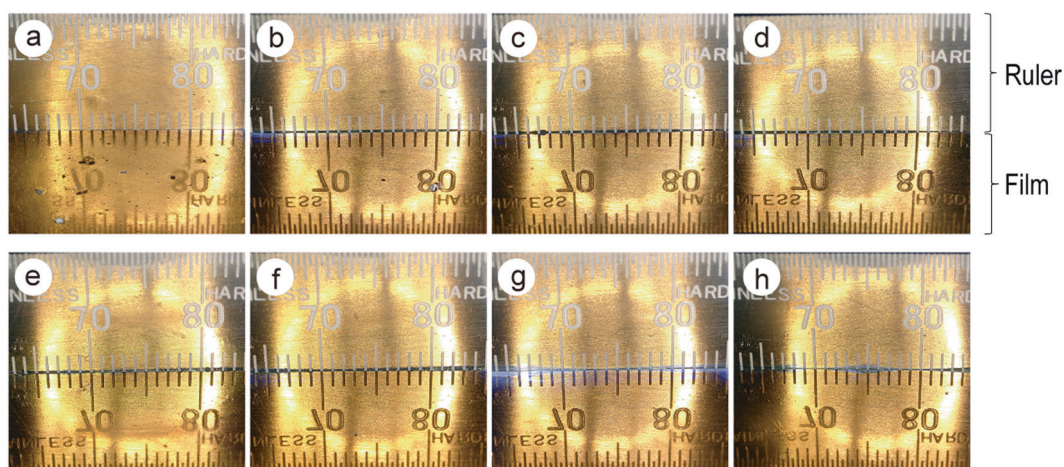


Fig. 4 Photographs of **a** Film(0.08, 10), **b** Film(0.08, 30), **c** Film(0.08, 60), **d** Film(0.08, 120), **e** Film(0.08, 60), **f** Film(10, 60), **g** Film(30, 60), and **h** Film(60, 60). The films in (c) and (e) were prepared from

O3MeOT synthesized under the same conditions using solution volumes of 70 and 100 μL , respectively. The bright ring in the images is due to the ring light source attached to the digital microscope

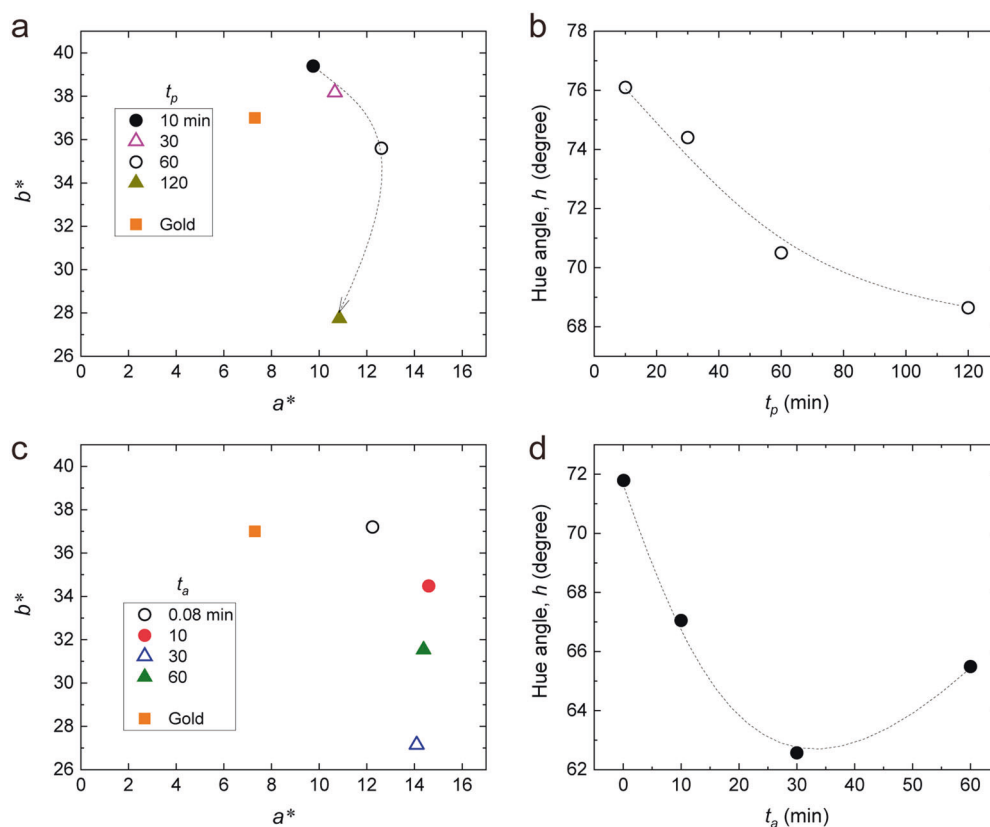


Fig. 5 **a**, **c** a^* , b^* chromaticity diagrams of films, with the diagram of a vacuum-evaporated gold film shown for comparison. Dependence of h on t_p (**b**) and t_a (**d**) for films

oligomer conjugation length. UV–vis absorption measurements of O3MeOT (Supplementary Fig. S2) showed interband absorption at 481 nm, and absorptions due to polaron and bipolaron bands caused by anion doping were observed above ~ 550 nm. With increasing doping level, the intensity of the former band decreases and that of the latter band

increases, which should contribute to color deepening. Table 2 shows film doping levels determined by scanning electron microscopy coupled with energy-dispersive X-ray spectrometry. Although the doping level of Film(0.08, 10) was smaller than those of films prepared at $t_p = 30, 60,$ and 120 min, the doping level was almost constant for

Table 2 Doping levels of O3MeOT films

Entry	Film	Doping level (%)
1	Film(0.08, 10) ^a	22
2	Film(0.08, 30) ^a	28
3	Film(0.08, 60) ^a	27
4	Film(0.08, 120) ^a	27
5	Film(0.08, 60) ^b	27
6	Film(10, 60) ^b	26
7	Film(30, 60) ^b	26
8	Film(60, 60) ^b	26

^aQuantity of the applied coating solution: 70 μ L

^bQuantity of the applied coating solution: 100 μ L

$t_p > 30$ min and could not account for the systematic changes in b^* and h seen in Fig. 5a, b, respectively. On the other hand, as the oligomer molecular weight, M_p , slightly increased with increasing t_p , the color deepening can be ascribed to the concomitant slight increase in conjugation length. However, the above interpretation should be treated with caution, as changes in b^* and h with t_p were small and the change in oligomer molecular weight was also small though meaningful.

Figure 5c, d shows the effects of t_a on film chromaticity and hue, respectively, revealing that the detected dependences were almost identical to those observed for t_p . However, the change in chromaticity with t_a was less pronounced and less systematic. The results reported in the previous section showed that the oligomer molecular weight decreased with increasing t_a , and Table 2 reveals that the oligomer doping level was almost constant irrespective of t_a . Therefore, film color deepening with increasing t_a could not be explained in terms of conjugation length and/or doping level changes. This behavior may reflect the difficulty of interpreting the chromaticity change due to its small range.

Reflection and structural properties of films

Specular reflection spectra were recorded to examine the film reflection color and reflectance. The reflection spectra of films prepared at $t_p = 10, 30, 60,$ and 120 min (t_a was held constant at 0.08 min) showed strong reflections of yellow (570–590 nm), orange (590–620 nm), and red (620–750 nm) light as well as slight reflections of green light (495–570 nm) (Fig. 6a). These characteristics were similar to those of evaporated metallic gold films and thus justified the gold-like appearances of oligomer films. The fact that all spectra near the reflection rising edge almost overlapped suggested that the wavelengths of these edges were almost equal (484 ± 5 nm). The maximum reflectance observed in the wavelength region of 600–700 nm was in the order of Film(0.08, 10) < Film(0.08, 120) < Film(0.08, 30) \approx Film(0.08, 60). Previously,

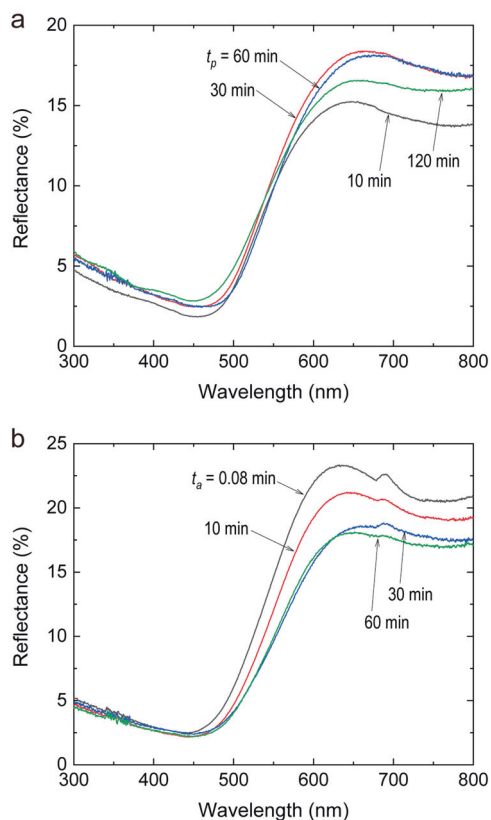
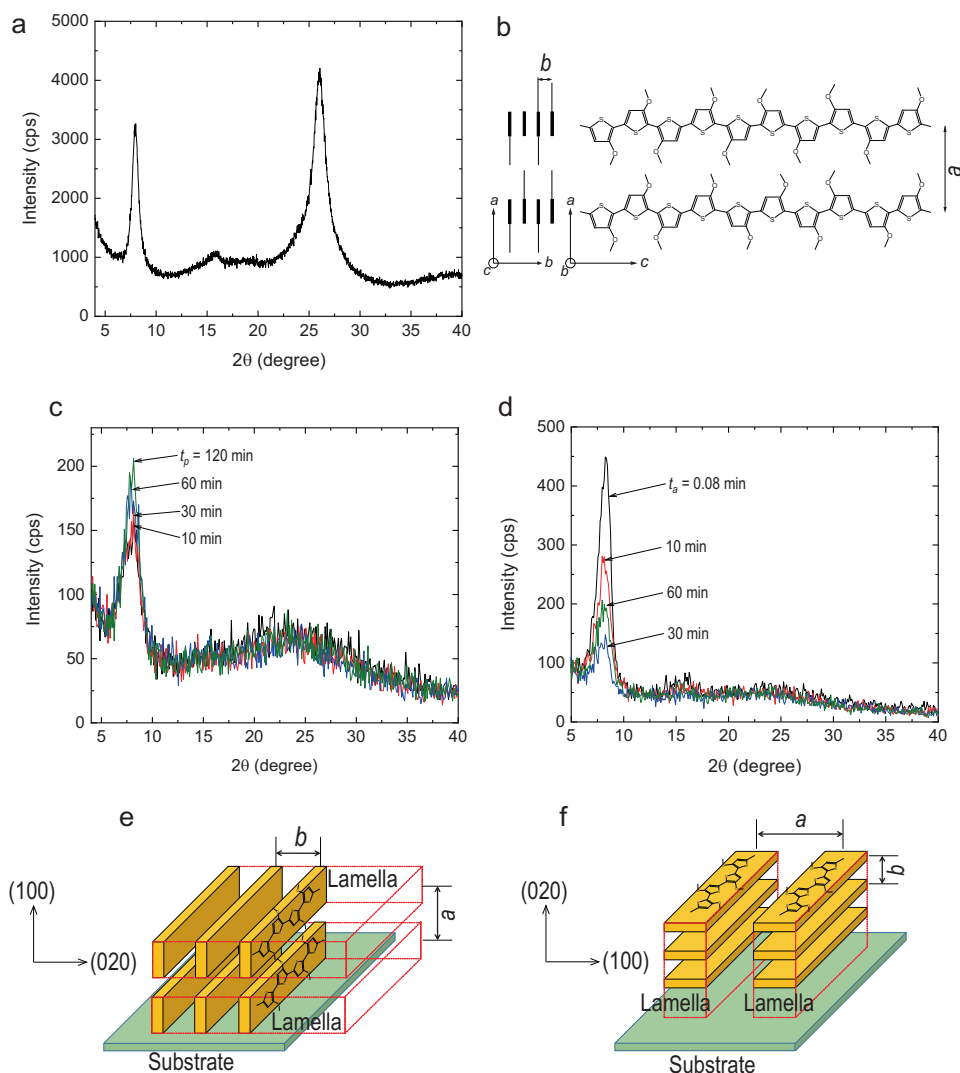


Fig. 6 Reflection spectra of **a** Film(0.08, t_p) ($t_p = 10, 30, 60,$ and 120 min) and **b** Film($t_a, 60$) ($t_a = 0.08, 10, 30,$ and 60 min). Note that films (0.08, 60) in (a) and films (0.08, 60) in (b) were prepared using coating solution volumes of 70 and 100 μ L, respectively

we reported that oligomer films contain two types of lamellar crystallites, namely, edge-on lamellar crystallites formed by arranging thiophene rings perpendicular to the substrate and face-on lamellar crystals formed by arranging rings parallel to the substrate and revealed that the former crystallites account for luster [15–17, 28]. Therefore, the formation of edge-on lamellar crystallites was probed by X-ray diffraction (XRD) analysis of oligomers and films.

The XRD pattern of O3MeOT(0.08, 60) showed signals at $2\theta = 7.41, \sim 15$ (shoulder), and 26.2° (Fig. 7a). The first two signals correspond to reflections from the (100) and (200) planes of lamellar crystallites, while the signal at 26.2° corresponds to reflection from the (020) plane of lamellar crystallites (Fig. 7b) [15–17]. The interlayer distances corresponding to $2\theta = 7.41^\circ$ and 26.2° were determined to be $a = 1.19$ nm and $b = 0.34$ nm, respectively. In the above pattern, the area of the signal corresponding to the (100) plane was close to that of the signal attributed to the (020) plane, which indicated the random orientation of the crystallites. However, in the case of films (Fig. 7c, d), the reflection from the (100) plane ($2\theta = 7.96^\circ, a = 1.11$ nm) was much stronger than that from the (020) plane, i.e., edge-on lamellar crystallites (Fig. 7e), in which

Fig. 7 **a** XRD pattern of O3MeOT(0.08, 60) powder. **b** Molecular arrangement of O3MeOT. XRD patterns of **c** Film(0.08, t_p) ($t_p = 10, 30, 60,$ and 120 min) and **d** Film($t_a, 60$) ($t_a = 0.08, 10, 30,$ and 60 min). Illustrations of **e** edge-on and **f** face-on lamellar crystallites



thiophene rings are oriented perpendicular to the substrate, were preferentially formed to face-on lamellar crystallites (Fig. 7f). Considering that the signal of the glass substrate ($2\theta = 23.47^\circ$) was superimposed on that at $2\theta \approx 25^\circ$, the intensity of the signal from the (020) plane was even lower, and hence, the dominance of edge-on lamellae was even more pronounced.

The XRD patterns of Film(0.08, t_p) ($t_p = 10, 30, 60,$ and 120 min) showed that the signal intensity at $2\theta = 7.96^\circ$ and, hence, the amount of edge-on lamellar crystallites, monotonously increased with increasing t_p (Fig. 7c). Previously, we reported that the amount of edge-on lamellar crystallites is positively correlated with film reflectance [16, 17, 28]. However, as shown in Fig. 6a, even though the crystal content was maximized at $t_p = 120$ min, the reflectance was not. To interpret this finding, we considered another factor affecting specular reflectance, namely, film surface roughness (R_q , Table 3). Film(0.08, 10) exhibited the lowest reflectance due to the smaller amount of edge-on lamellar

Table 3 Film thickness, d , root mean square surface roughness, R_q , and electric conductivity, σ , of the O3MeOT films

Entry	Film	d (μm)	R_q (μm)	$10^2 \sigma$ (S cm^{-1})
1	Film(0.08, 10) ^a	1.7	0.322	0.44
2	Film(0.08, 30) ^a	1.8	0.024	0.97
3	Film(0.08, 60) ^a	1.5	0.051	4.7
4	Film(0.08, 120) ^a	1.7	0.116	3.3
5	Film(0.08, 60) ^b	2.5	0.052	2.2
6	Film(10, 60) ^b	2.7	0.021	1.3
7	Film(30, 60) ^b	2.5	0.023	0.20
8	Film(60, 60) ^b	2.6	0.044	0.60

^aQuantity of the applied coating solution: 70 μL

^bQuantity of the applied coating solution: 100 μL

crystallites and the roughest surface with $R_q = 0.322$, which was one order of magnitude larger than the values of Film(0.08, 30) and Film(0.08, 60). This behavior should be ascribed to the poor film-forming properties of O3MeOT

(0.08, 10) arising from its lower average molecular weight. Although not clearly seen in Fig. 4d, fine wrinkle-like structures were observed in Film(0.08, 120), possibly because of its relatively high crystallinity, and probably contributed to the relatively large R_q of 0.116. Benett et al. reported that the following relationship between R_q and specular reflectance R_s holds when the light of wavelength λ is incident on a plane with a surface roughness of R_q at an angle θ to the normal under the condition of $R_q \ll \lambda$ [29].

$$R_s = R_0 \exp \left\{ -16(\pi R_q)^2 / \lambda^2 \right\} + 2^5 \pi^4 R_0 R_q^4 (\Delta\theta)^2 / (m^2 \lambda^4) \quad (2)$$

where R_0 , m , and $\Delta\theta$ are the reflectance of a perfectly smooth surface, the root mean square slope of the surface profile, and the instrumental acceptance angle ($\Delta\theta \approx 0.1$ rad for the instrument employed herein), respectively. Herein, R_s/R_0 could not be calculated, as the value of m was unknown. However, the reports in which Eq. (2) was applied to glass and metal surfaces [30, 31] indicated that R_s/R_0 monotonically decreased with R_q when R_q was in the range of values listed in Table 3. Therefore, the fact that the reflectance of Film(0.08, 120) was not the highest (see Fig. 6a) may be ascribed to its large R_q .

Figure 6b shows the specular reflection spectra of Film(t_a , 60) ($t_a = 0.08, 10, 30$, and 60 min), revealing that the wavelength corresponding to the onset of reflectance rise increased with increasing t_a and equaled 480, 486, 491, and 491 nm for $t_a = 0.08, 10, 30$, and 60 min, respectively. This behavior could be ascribed to the concomitant increase in the conjugation length of oligomer molecules, although this assumption is incompatible with the decrease in M_p with t_a (see Table 1). Furthermore, as shown in Table 2, the film doping level (discussed above) was almost constant regardless of t_a and could therefore not be held responsible for the redshift. The maximum reflectances in the range of 600–700 nm were in the order of Film(30, 60) \approx Film(60, 60) < Film(10, 60) < Film(0.08, 60). The corresponding XRD patterns (Fig. 7c) showed that the intensity of the signal at $2\theta = 7.96^\circ$ was in the order Film(30, 60) < Film(60, 60) < Film(10, 60) < Film(0.08, 60). Although the order of reflectance at $t_a = 30$ min and 60 min was reversed, the reflectance showed a tendency to decrease with increasing t_a . As R_q was almost independent of t_a (see Table 3), this result supports the previously observed increase in specular reflectance with increasing content of edge-on lamellar crystallites in the film [16, 17, 28].

Note that the scale of the vertical axis in Fig. 7d is different from that in Fig. 7c because of the different thicknesses of the film samples (see Table 3). Furthermore, one should note that the change in intensity at $2\theta = 7.96^\circ$ in Fig. 7d is much larger than that in Fig. 7c, which cannot be

explained only by the difference in film thickness and indicates that during oligomer synthesis, the effect of t_a on film crystallinity is much larger than that of t_p . Herein, we found that t_a and t_p did not strongly affect the oligomer doping level but exerted a discernible influence on molecular weight. This influence was more pronounced for t_a than for t_p and was presumably linked to the extent of the change in film crystallinity. In turn, the crystallinity of films may affect the intensity and wavelength dependence of their optical constant (refractive index and extinction coefficient) spectra and thus influence optical properties such as reflectance, reflectance rise threshold, and color. The polymerization degree of thiophene-based polymers is roughly determined by the employed solvent (acetonitrile in our case) [27]. Nevertheless, changes in t_p and t_a can be assumed to affect the molecular weight and, hence, film structural and optical properties. Considering the modest change in molecular weight, the sensitivity of film structural and optical properties to this parameter was concluded to be very large.

Electric conductivity of films

In poly(3-alkylthiophene) films, charge mobility in the direction parallel to the (020) axis exceeds that in the direction parallel to the (100) axis [32–34]. Consequently, for films with a dominant edge-on orientation (Fig. 7e), charge carrier mobility is higher in the π - π stacking direction, which is parallel to the substrate surface. In fact, for poly(3-hexylthiophene) films with thiophene rings oriented edge-on to the substrate, the in-plane electric conductivity was reported to be 19–950 times higher than that in the film thickness direction (anisotropic conduction) [34]. The electropolymerization of 3-methoxythiophene was used to prepare films with dominant edge-on and face-on lamellae, and the in-plane electrical conductivity of the former films was reported to be 1.5×10^3 times higher than that of the latter films [35]. Moreover, electric conductivity in the in-plane direction is positively correlated with the crystallinity of edge-on lamellae [34]. More importantly, the degree of crystallinity and hence charge mobility increases with increasing molecular weight [36–39].

Therefore, the electric conductivity (σ) of films was measured to confirm whether the above general behavior of poly(3-alkylthiophene)s is also valid for O3MeOT (Supplementary Fig. S3). The rightmost column of Table 3 shows the σ values of each film, revealing that similar to M_p and the amount of edge-on lamellar crystallites, σ increased with increasing t_p . Based on the above, we concluded that the oligomer molecular weight and, hence, the degree of crystallinity and conductivity increased with increasing t_p . On the other hand, σ decreased with increasing t_a . Given that both M_p and the amount of edge-on lamellar crystallites

exhibited a negative correlation with t_a , the increase in t_a probably resulted in a decrease in oligomer molecular weight and hence in a reduction in crystallinity and σ . Thus, the conductivities of the prepared O3MeOT samples agreed with the correlation between the molecular weight, crystallinity, and conductivity of poly(3-alkylthiophene)s.

Conclusions

This study probed the effects of oxidant addition time t_a and polymerization time t_p on the physicochemical properties of oligo(3-methoxythiophene) and the corresponding solution-cast films. The oligomer molecular weight, amount of edge-on lamellar crystallites in films, and film conductivity were negatively correlated with t_a and positively correlated with t_p . In addition, film reflectance depended on the amount of edge-on lamellar crystallites and film surface roughness. These correlations provide a guideline for controlling the metal-like luster of films and were concluded to be important from the perspective of color engineering. Thus, gloss and chromaticity could be simply tuned by controlling t_a and/or t_p to expand the range of oligomer applications as paints and inks.

Moreover, the above findings rely on the concepts of molecular orientation and electrical conductivity and thus contribute to the development of organic electronics similar to those based on poly(3-alkylthiophene)s. Currently, we plan to study the effect of polymerization temperature on film gloss and chromaticity to further extend the control range.

Acknowledgements This work was financially supported by JSPS KAKENHI Grant Number 20K05614. The authors thank the Center for Analytical Instrumentation of Chiba University for measurements of the specular reflection and ^1H NMR spectra.

Compliance with ethical standards

Conflict of interest The authors declare no competing interests.

Publisher's note Springer Nature remains neutral with regard to jurisdictional claims in published maps and institutional affiliations.

References

1. Granström M. Novel polymer light-emitting diode designs using poly(thiophenes). *Polym Adv Technol*. 1997;8:424–30.
2. Bento DC, Maia ECR, Cervantes TNM, Fernandes RV, Mauro ED, Laureto E, et al. Optical and electrical characteristics of poly(3-alkylthiophene) and polydiphenylamine copolymers: applications in light-emitting devices. *Synth Met*. 2012;162:2433–42.
3. Bao Z, Dobabalapur A, Lovinger AJ. Soluble and processable regioselective poly(3-hexylthiophene) for thin film field-effect transistor applications with high mobility. *Appl Phys Lett*. 1996;69:4108–10.
4. Huynh WU, Dittmer JJ, Alivisatos AP. Hybrid nanorod-polymer solar cells. *Science*. 2002;295:2425–7.
5. Kim Y, Cook S, Stelios Choulis SA, Nelson J, Durrant JR, Donal, et al. Organic photovoltaic devices based on blends of regioregular poly(3-hexylthiophene) and poly(9,9-dioctylfluorene-cobenzothiadiazole). *Chem Mater*. 2004;16:4812–8.
6. Fukuda H, Yamagishi Y, Isea M, Takano N. Gas sensing properties of poly-3-hexylthiophene thin film transistors. *Sens Actuators B*. 2005;108:414–7.
7. Yoshino K, Hayashi S, Sugimoto R. Preparation and properties of conducting heterocyclic polymer films by chemical method. *Jpn J Appl Phys*. 1984;23:L899–L900.
8. Leclerc M, Diaz FM, Wegner G. Structural analysis of poly(3-alkylthiophene)s. 1989;190:3105–16.
9. Chen TA, Wu X, Rieke RD. Regiocontrolled synthesis of poly(3-alkylthiophenes) mediated by Rieke zinc: Their characterization and solid-state properties. *J Am Chem Soc*. 1995;117:233–44.
10. Facchinatto WM, Torres BB, Balogh DT. One-pot synthesis of poly(3-hexylthiophene) with variable degrees of molar mass and regioregularity. *J Polym Res*. 2016;23:187.
11. Torres BBM, Balogh DT. Regioregular improvement on the oxidative polymerization of poly-3-octylthiophenes by slow addition of oxidant at low temperature. *J Appl Polym Sci*. 2012;124:3222–8.
12. Andersson MR, Selse D, Berggren M, Järvinen H, Hjertberg T, Inganäs T, et al. Regioselective polymerization of 3-(4-octylphenyl)thiophene with FeCl_3 . *Macromolecules*. 1994;27:6503–6.
13. Amou S, Haba O, Shirato K, Hayakawa T, Ueda M, Takeuchi K, et al. Head-to-tail regioregularity of poly(3-hexylthiophene) in oxidative coupling polymerization with FeCl_3 . *J Polym Sci Pol Chem*. 1999;37:1943–8.
14. Shimomura M, Kaga M, Nakayama N, Miyauchi S. Thermal and electrical properties of poly(3-alkylthiophene)s prepared by the oxidative polymerization. *Synth Met*. 1995;69:313–4.
15. Tagawa R, Masu H, Itoh T, Hoshino K. Solution-cast self-assembled films of perchloratedoped oligo(3-methoxythiophene) showing a gold-like luster. *RSC Adv*. 2014;4:24053–8.
16. Takashina Y, Mitogawa T, Saito K, Hoshino K. Chemical events in oligo(3-methoxythiophene) coating solutions and their effect on the goldlike coating film properties. *Langmuir*. 2018;34:3049–57.
17. Takashina Y, Hoshino K. Effect of π - π interaction-induced secondary doping on the gold-like luster of oligo(3-methoxythiophene) cast films. *Polym J*. 2019;51:591–9.
18. Hill MG, Penneau JF, Zinger B, Mann KR, Miller LL. Oligothiophene cation radicals. π -dimers as alternatives to bipolarons in oxidized polythiophenes. *Chem Mater*. 1992;4:1106–13.
19. Hill MG, Mann KR, Miller LL, Penneau JF. Oligothiophene cation radical dimers. An alternative to bipolarons in oxidized polythiophene. *J Am Chem Soc*. 1992;114:2728–30.
20. Yu Y, Gunic E, Zinger B, Miller LL. Spectra and reactivity of methoxyoligothiophene cation radicals. *J Am Chem Soc*. 1996;118:1013–8.
21. D'agnillo L, Soares JBP, Penlidis A. Round-robin experiment in high-temperature gel permeation chromatography. *J Polym Sci B*. 2002;40:905–21.
22. Zhang ZB, Fujiki M. Synthesis and molecular weight dependent optical properties of mono-alkoxy substituted polythiophenes. *Polym J*. 2001;33:597–601.
23. Hu X, Xu L. Structure and properties of 3-alkoxy substituted polythiophene synthesized at low temperature. *Polymer*. 2000;41:9147–54.

24. Mao H, Holdcroft S. Grignard synthesis of π -conjugated poly(3-alkylthiophenes): Controlling molecular weights and the nature of terminal units. *Macromolecules*. 1992;25:554–8.
25. Mao H, Xu B, Holdcroft S. Synthesis and structure-property relationships of regioirregular poly(3-hexylthiophenes). *Macromolecules*. 1993;26:1163–9.
26. Barbarella G, Bongini A, Zambianchi M. Regiochemistry and conformation of poly(3-hexylthiophene) via the synthesis and the spectroscopic characterization of the model configurational triads. *Macromolecules*. 1994;27:3039–45.
27. Barbarella G, Zambianchi M, Rosanna Toro RD, Colonna M Jr, Iarossi D, Francesca Goldoni F, et al. Regioselective oligomerization of 3-(alkylsulfanyl)thiophenes with ferric chloride. *J Org Chem*. 1996;61:8285–92.
28. Tachiki M, Tagawa R, Hoshino K. Oligo(3-methoxythiophene)s as water-soluble dyes for highly lustrous gold- and bronze-like metal-effect coatings and printings. *ACS Omega*. 2020;5:24379–88.
29. Bennett HE, Porteus JO. Relation between surface roughness and specular reflectance at normal incidence. *J Opt Soc Am*. 1961;51:123–9.
30. Dobierzewska-Mozrzyms E, Rysiakiewicz-Pasek E, Bieganski P, Polanska J, Pieciul E. Application of the optical method for determining of the RMS roughness of porous glass surfaces. *J Non-Cryst Solids*. 2008;354:3241–5.
31. Ohara M, Takigawa Y, Higashi K. Effect of surface roughness on specular gloss in AZ31 magnesium alloy. *J Jpn Inst Light Met*. 2010;60:259–63.
32. Siringhaus H, Tessler N, Richard H, Friend RH. Integrated optoelectronic devices based on conjugated polymers. *Science*. 1998;280:1741–4.
33. Siringhaus H, Brown PJ, Friend RH, Nielsen MM, Bechgaard K, Langeveld-Voss BMW, et al. Two-dimensional charge transport in self-organized, high-mobility conjugated polymers. *Nature*. 1999;401:685–8.
34. Liu C, Oshima K, Masato Shimomura M, Miyauchi S. Anisotropic conductivity–temperature characteristic of solution-cast poly(3-hexylthiophene) films. *Synth Met*. 2006;156:1362–7.
35. Tokuda T, Hoshino K. Electropolymerized films of 3-methoxythiophene with a potential sweep-induced gold-like luster. *Polym J*. 2016;48:1141–9.
36. Kline RJ, McGehee MD, Kadnikova EN, Liu J, Fréchet JMJ, Toney MF. Dependence of regioregular poly(3-hexylthiophene) film morphology and field-effect mobility on molecular weight. *Macromolecules*. 2005;38:3312–9.
37. Kline RJ, McGehee MD, Kadnikova EN, Liu J, Fréchet JMJ. Controlling the field-effect mobility of regioregular polythiophene by changing the molecular weight. *Adv Mater*. 2003;15:1519–22.
38. Zen A, Pflaum J, Hirschmann S, Zhuang W, Jaiser F, Asawaprom U, et al. Effect of molecular weight and annealing of poly(3-hexylthiophene)s on the performance of organic field-effect transistors. *Adv Funct Mater*. 2004;14:757–64.
39. Zen A, Saphiannikova M, Neher D, Grenzer J, Grigorian S, Pietsch U, et al. Effect of molecular weight on the structure and crystallinity of poly(3-hexylthiophene). *Macromolecules*. 2006;39:2162–71.